Vol. 4 No. 1 page 34-40
DOI: .....

RESEARCH & KNOWLEDGE

Research Article

Fe_3O_4@Ag core-shell composite nanoparticle with tunable optical property

Thananchai Dasri[1] and Artit Chingsungnoen[2,*]

[1]Faculty of Applied Science and Engineering, Khon Kaen University, Khon Kaen 40002, Thailand
[2]Technological Plasma Research Unit, Department of Physics, Faculty of Science, Mahasarakham University, Maha Sarakham 44150, Thailand

(Received 24 May 2017; accepted 12 July 2017)

Abstract - In this work, plasmonic behaviors exhibited by nanoparticles (NP) composed of magnetite (Fe_3O_4) cores with silver (Ag) shells were investigated by discrete dipole approximation (DDA). First, the Fe_3O_4 core size was fixed at 32 nm and the Ag shell thickness was varied from 8 nm to 15 nm. Second, the Ag shell thickness was fixed at 16 nm and the Fe_3O_4 core diameters were between 5 and 20 nm. The calculated absorption peaks showed two peaks positioned to the left and right of 382 nm, which is the peak position of pure Ag. The results revealed that by varying either the Fe_3O_4 core size or the Ag shell thickness compared with pure Fe_3O_4 and Ag NP, light absorption enhancement and tunable aspects are successfully achieved. This nanomaterial is expected to be applicable in biomedicine, nanocatalysis, optic devices, and new functional devices in the future.

Keywords: Iron oxide-silver nanoparticles, surface plasmon resonance, discrete dipole approximation

1. Introduction

Typical nanosized magnetic particles of magnetite, Fe_3O_4, have been found to be highly applicable in various fields, especially in biology and medicine, for example, as contrast agents for magnetic resonance imaging (MRI) and drug delivery (Arbab *et al*., 2003; Cunningham *et al*., 2005; Mahmoudi *et al*., 2011; Jiang *et al*., 2012; Kim *et al*., 2018). Fe_3O_4 chemically contains both Fe^{2+} and Fe^{3+}, in which the electron configuration of the Fe^{3+} ion is $1s^2\ 2s^2\ 2p^6\ 3s^2 3p^6 3d^5$ and the Fe^{2+} ion is $1s^2\ 2s^2\ 2p^6\ 3s^2\ 3p^6\ 3d^6$. Consequently, it is the Fe 3d electrons that determine the electronic, magnetic, and some spectroscopic properties. This is an inverse spinel structure with oxygen forming a face-centered cubic closed packing structure and Fe cations occupying interstitial tetrahedral and octahedral sites (Sheng-Nan *et al*., 2014). However, this component is the only part of the Fe_3O_4 nanoparticles that does not show strong absorption of visible electromagnetic (EM) spectrum (Lim *et al*., 2008; Armelles *et al*., 2013). Currently, employing optical resonances of noble metals, such as gold (Au), silver (Ag), and copper (Cu), nanostructures have been utilized for enhancing and tuning optical and magneto-optical phenomena (Jiang *et al*., 2012; Lim *et al*., 2008; Armelles *et al*., 2013; Brollo *et al*., 2014; Jain *et al*., 2009; Yang *et al*., 2015; Chaiyachate and Dasri, 2017; Dasri, 2016). Moreover, this composite nanoparticle (NP) shows good magnetic and electrical properties (Sun *et al*., 2012). These metals with their sizes are recognized for supporting localized surface plasmon resonance (LSPR), which results in a strong absorption and scattering feature as well as near-field enhancements at plasmon resonance in the near ultraviolet (UV) to near infrared (NIR) of the EM spectrum. LSPR are collective oscillating gas electrons with respect to a fixed lattice of positive ions with a resonant frequency that depends on geometrical, compositional parameters, and dielectric properties of the surrounding medium (Jain *et al*., 2009; Yang *et al*., 2015). In addition, complex applications, especially in biomedicine, require multicomponent materials in a single nanoparticle due to these combined materials being expected to provide an improved performance. In addition, the use of magnetic material, such as Fe_3O_4, combined with plasmonic material has attracted the attention of the scientific community, especially when there are spherical composites of magnetic material as the core and plasmonic material as the shell, or vice versa (Jiang *et al*., 2012; Lim *et al*., 2008; Armelles *et al*., 2013; Brollo *et al*., 2014; Jain *et al*., 2009; Yang *et al*., 2015; Chaiyachate and Dasri, 2017; Dasri, 2016). Recently, experimental work (Jiang *et al*., 2012; Brollo *et al*., 2014) has successfully fabricated super-paramagnetic Ag@Fe_3O_4 core-shell nanospheres for use in biomedical applications. This article only gives the optical absorption properties for the multicomponent Fe_3O_4@Ag core-shell nanoparticle embedded in water as it will be investigated from simulations. Ag was selected because it provides a higher optical enhancement (Sompech *et al*., 2016). Moreover, the transition of an electron from the 4d→5s state exhibits plasmon resonance in the far ultra-

*Author for correspondence: artit.ching@gmail.com

violet region and shifts it to the visible region of the EM spectrum[16]. The surface plasmon resonance indicated that it can be enhanced and tuned by adjusting the core size and shell thickness of the composite particles. This study will contribute to a better understanding of the optical properties that can be obtained from the construction or synthesis the Fe_3O_4@Ag core-shell bifunctional nanostructures for the associated applications.

2. Computational details

Discrete dipole approximation (DDA) is a numerical method for calculating the optical properties of materials by approximating them with each nanoparticle represented by a point dipole (Purcell and Pennypacker, 1973). As soon as the coordinates and polarizabilities of the individual dipoles are known, the scattering, extinction, and absorption properties of the whole structure can be solved exactly. In this method, the object of interest is divided into N point dipoles whose positions are denoted $\vec{r}_i$ with polarizability tensor $\tilde{\alpha}_i$. The polarization of the i^{th} element due to interactions with a local electric field $\vec{E}_{loc,i}$ will be as follows:

$$\vec{P}_i = \alpha_i \vec{E}_{loc}(\vec{r}_i), \quad (1)$$

where $\tilde{\alpha}_i$ is the polarizability tensor of the nanoparticle describing its dipole response to the external electric field. For isolated particles, the local electric field $\vec{E}_{loc,i}$ is the sum of the incident field and a contribution from all the other dipoles in the same particle:

$$\vec{E}_{loc,i} = \vec{E}_{inc,i} - \sum_{i \neq j} \tilde{A}_{ij} \vec{P}_j, \quad (2)$$

where the first term, $\vec{E}_{inc,i}$, is the incident radiation field and the second term is the contributions of other $N-1$ dipoles. The electric field $\tilde{A}_{ij}\vec{P}_j$ at the position $\vec{r}_i$ has the following form:

$$\tilde{A}_{ij}\vec{P}_j = \frac{e^{ikr_{ij}}}{r_{ij}^3}[k^2\vec{r}_{ij}\times(\vec{r}_{ij}\times\vec{P}_j) + \frac{(1-ikr_{ij})}{r_{ij}^2}\times(r_{ij}^2\vec{P}_j - 3\vec{r}_{ij}(\vec{r}_{ij}\cdot\vec{P}_j)], \; i \neq j, \quad (3)$$

where $k = \frac{2\pi}{\lambda}\sqrt{\varepsilon_m}$ is the wave vector of the incident light and ε_m is the dielectric constant of the surrounding medium. For N particles, by substituting Eqs. (2) and (3) into Eq. (1), the polarizations of each particle $\vec{P}_j$ can be solved. Later, the extinction and absorption cross sections are obtained as follows:

$$C_{ext} = \frac{4\pi k}{|E_0|^2}\sum_{i=1}^{N} \mathrm{Im}(\vec{E}^*_{inc,i}\cdot\vec{P}_j), \quad (4)$$

$$C_{abs} = \frac{4\pi k}{|E_0|^2}\sum_{i=1}^{N}\{\mathrm{Im}(\vec{P}_i\cdot(\tilde{\alpha}_i^{-1})^*\vec{P}_i^*) - \frac{2}{3}k^3|\vec{P}_i|^2\}. \quad (5)$$

By using these equations, the scattering cross sections can be obtained using $C_{scat} = C_{ext} - C_{abs}$. For a composite nanoparticle assumed to be spherical, with a Fe_3O_4 core (ε_c) of radius b, surrounded by a shell of gold (ε_b) to outer radius a, much less than the wavelength of the light is considered. The composite particle's dielectric function ε_s is found to be (Dani *et al*., 2011) :

$$\varepsilon_s = \varepsilon_b\frac{1+2\beta_c}{1-\beta_c}, \; \beta_c = f_c\frac{\varepsilon_c-\varepsilon_b}{\varepsilon_c+2\varepsilon_b}, \quad (6)$$

where $f_c = (b/c)^3$ is the internal volume fraction. Eventually, the absorption cross sections can be calculated using Eq. (3). In this calculation, the dielectric constants for Fe_3O_4 were taken from Fontijn *et al*. (1997) [19]. The Fe_3O_4 @Ag core-shell NP size was taken from Lim and co-workers (Brollo *et al*., 2014)[9]. The dielectric constants for metal NPs were extracted from the experimental results in Johnson and Christy (1972) [20]. The dielectric constant of water was used as the surrounding medium and is 1.77.

3. Results and discussion

The optical properties of the pure Fe_3O_4 and Ag as well as the Fe_3O_4@Ag core-shell nanostructures were investigated by DDA calculation in the UV-near infrared region of the EM spectrum with the results shown in Figures 1-4. As mentioned, the Ag NP was utilized as a nanoshell for supporting the SPR due to it exhibiting a more intense SPR for the EM wave in the visible light region. Figure 1a shows the absorption spectrum of the Ag NP when compared with that obtained from the Au NP. While the LSPR peaks were found at ~382 nm and ~522 nm for Ag and Au, respectively. Moreover in Figure 1b and 1c, the absorption spectra of the bare Fe_3O_4 and Ag nanoparticles (NPs) are also presented for reference. The absorption spectra of different Fe_3O_4 sizes from 6 nm to 20 nm exhibited no obvious absorption peaks in the visible region, as shown in Figure 1b. On the other hand, the absorption spectrum of the Ag NP shows a strong LSPR peak. LSPR peaks were found at ~382 nm for all particles with sizes from 6 nm to 20 nm. After coating the Fe_3O_4 NP with an Ag nanoshell, the absorption spectra shown in Figures 2-4 were obtained. Figure 2 shows the calculated absorption cross sections of Fe_3O_4@Ag core-shell NPs with a uniform 16 nm Fe_3O_4 core and 15 nm Ag shell thickness in water.

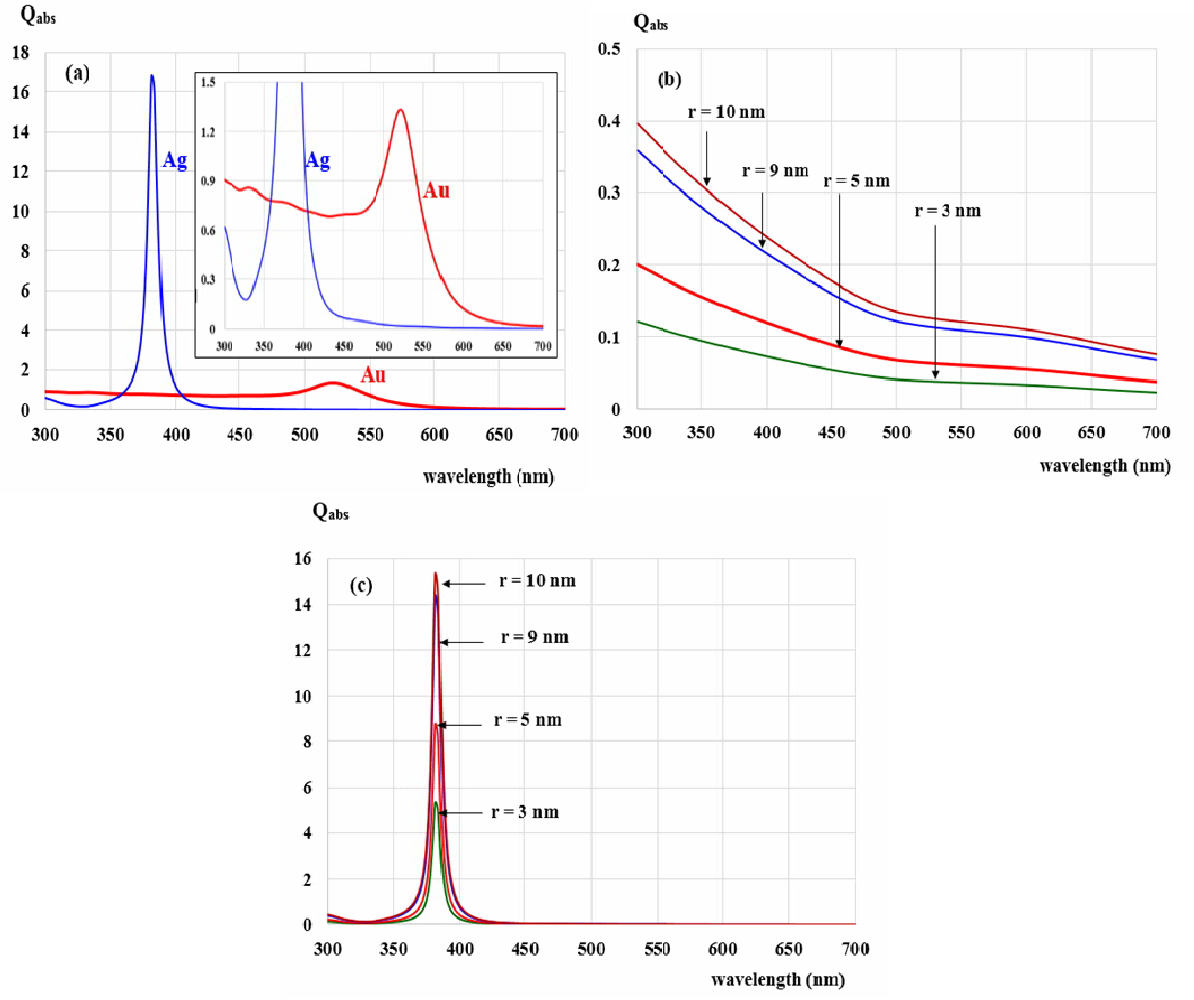

Figure 1. Calculated absorption efficiency of (a) Ag compared with Au, (b) pure Fe_3O_4 with various particle sizes, and (c) pure Ag with various particle sizes embedded in water.

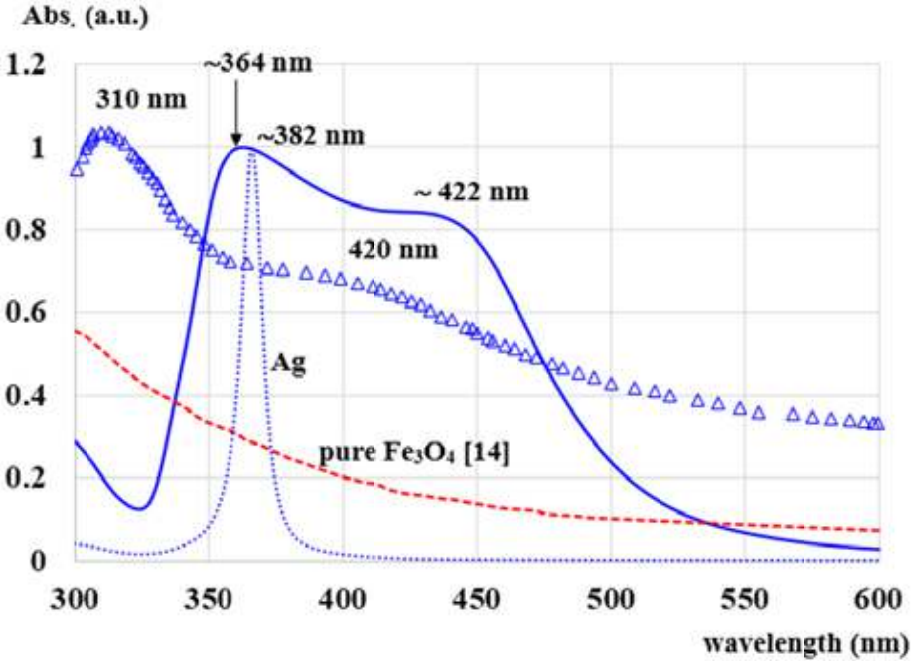

Figure 2. Calculated absorption spectra of Fe_3O_4 @Ag composite particle (solid line) compared with two experimental spectra (adapted from Sun *et al*., 2012) and Ag nanoparticle with particle size of 10 nm. Experimental spectra consist of spectra of pure Fe_3O_4 (dash line) and Fe_3O_4 @Ag core-shell spectra obtained from reaction times of 1 hour (triangle line).

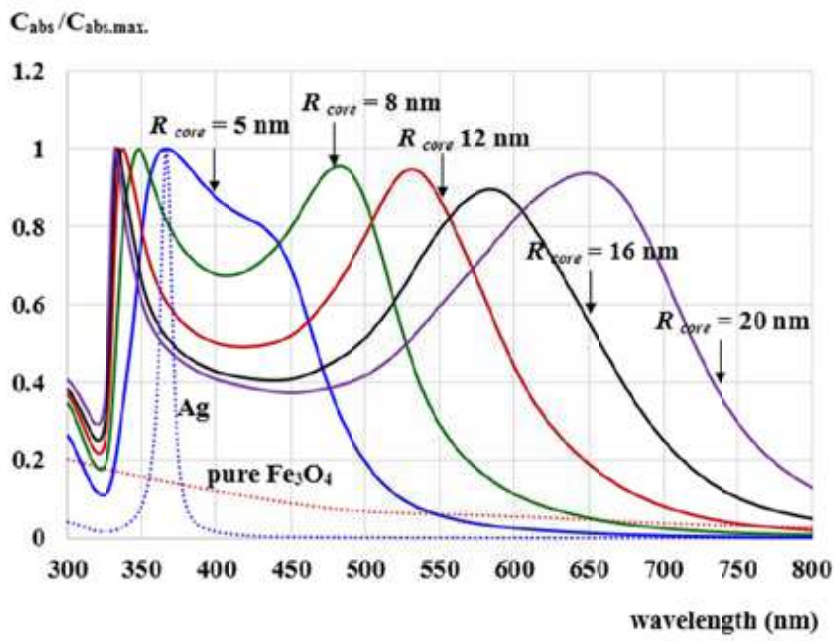

Figure 3. Calculated absorption spectra of Fe_3O_4 @Ag composite particle with fixed Ag shell thickness of 5 nm. Fe_3O_4 core radius (R_{core}) was varied from 5 nm to 20 nm.

The LSPR positions were found at ~364 nm and ~422 nm, which are on the left and right sides of the LSPR position obtained from pure Ag (~382 nm), respectively. Compared with the pure Ag spectrum, the ~382 nm LSPR peak position, it was found that they shifted to shorter (near UV) and longer wavelengths (blue of visible light) for the first and second peaks, respectively. In addition, experimental results adapted from Sun *et al*. (2012) were taken as a comparison with our results. Comparing the first observation with the pure Fe_3O_4 spectrum, it was clear that the coating of the Ag nanoshell influenced the light absorption enhancement. Moreover, the trend line of the calculated spectrum looked like the two lines of the experimental results. The second LSPR positions of both the calculated and the experimental results were found around 420 nm. However, the Fe_3O_4/Ag core-shell composite NPs in Sun *et al*. (2012) were prepared with different reaction times of 10 min (diamond line) and 1 hour (triangle line). Moreover, the transmission electron microscopy (TEM) images of the Fe_3O_4 @Ag composite NPs, which this group synthesized, did not show uniform particle sizes. Figure 3 shows the absorption spectra of the Fe_3O_4 @Ag composite particle with a fixed Ag shell thickness of 5 nm. For the LSPR position on the left side of 382 nm (LSPR position of pure Ag), when the Fe_3O_4 core radius increased from 5 nm to 20 nm, it was found that the LSPR position slightly shifted until it reached ~332 nm for a 20 nm Fe_3O_4 core. Whereas, the second peak for the LSPR on the right side of 382 nm showed a longer wavelength shifting. It shifted to ~422, ~482, ~532, ~584, and ~650 nm for 5, 8, 12, 16, and 20 nm Fe_3O_4 core radii, respectively. It was observed that the relation between the LSPR position (λ_{max}) and Fe_3O_4 core radius (R_{core}) was linear as $\lambda_{max}[\text{nm}] = 14.641R_{core} + 355.38$, as shown in Figure 4. In addition, it was clear that the coating of the plasmonic material nano-shell showed light absorption enhancement corresponding to previous experimental results (Brollo *et al*., 2014; Sun *et al*., 2012).

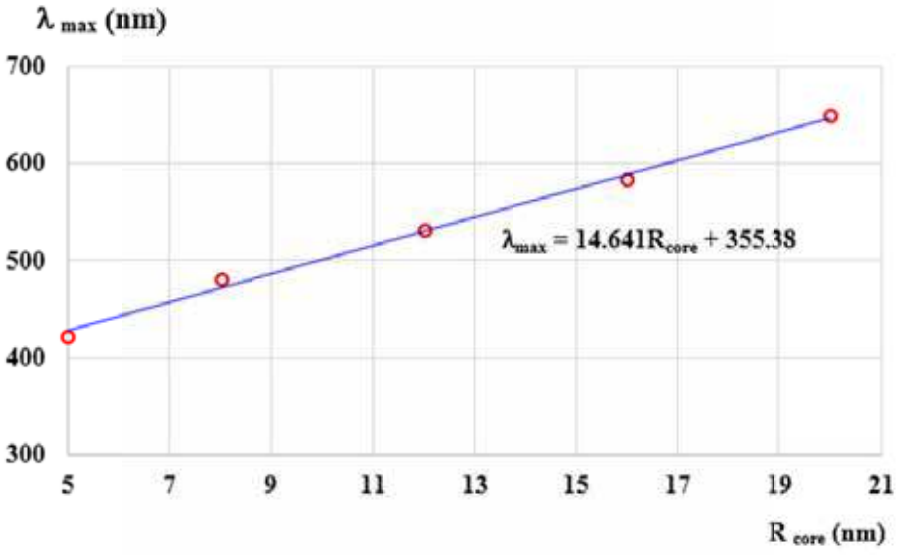

Figure 4. Relationship between LSPR position and Fe_3O_4 core radius.

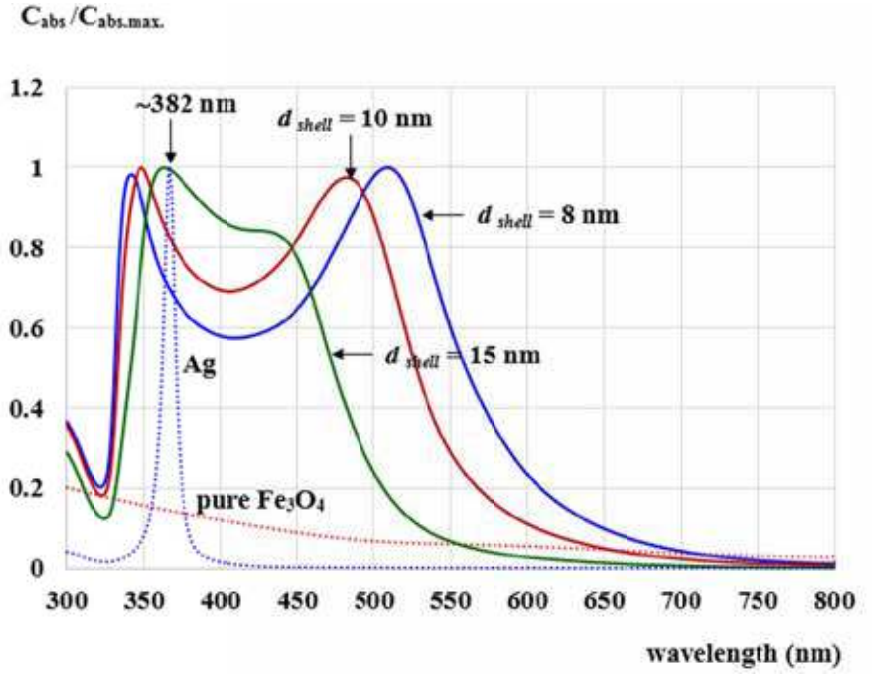

Figure 5. Calculated absorption spectra of Fe_3O_4 @Ag composite particle with fixed Fe_3O_4 core radius (R_{core}) of 16 nm. The Ag shell thickness (d_{shell}) was varied from 8 nm to 15 nm.

Additional calculations of the plasmonic spectra with increasing Ag shell thicknesses, as shown in Figure 5, had the absorption spectra of three Fe_3O_4 @Ag composite NPs with a fixed Fe_3O_4 core radius of 16 nm, and they were compared with the pure Fe_3O_4 spectrum. These samples were coated with different thicknesses of Ag shells consisting of 8 nm, 10 nm, and 15 nm. For the LSPR peak on the right side of 382 nm, it was found that after coating the Fe_3O_4 with the Ag nanoshell, the light could be enhanced. It had shifts in the LSPR peak positions to ~424 nm, ~482 nm, and ~508 nm for the shell thicknesses of 15 nm, 10 nm, and 8 nm, respectively. On the other hand, the LSPR peak on the left side of 382 nm slightly shifted to a shorter wavelength as the shell thickness decreased. It shifted to ~362, ~348, and ~342 nm for the shell thicknesses of 15 nm, 10 nm and 8 nm, respectively. In comparison with pure Fe_3O_4, the calculated absorption spectra were observed to enhance the light absorption when coating the Fe_3O_4 with a plasmonic nanomaterial (i.e., Ag). Moreover, the LSPR peak position could be tuned by varying both the Fe_3O_4 core sizes and plasmonic material shell thickness. They were in good agreement with the experimentally determined values in terms of the LSPR peak position at any dimension of the sample, the enhancement of light absorption, and the changes in the LSPR peak position as a function of either the Fe_3O_4 core size or the

Ag shell thickness Lim *et al*., 2008; Jain *et al*., 2009; Sun *et al*., 2012). The explanation of the physical aspects behind the LSPR peak position change, as developed by Prodan et al., relied on the plasmon modes coupling theory (Prodan and Nordlander, 2003; 2004). In this theory, the metallic sphere plasmon exhibited from the outer surface of the metallic shell layer coupled with the cavity plasmons produced from the inner metallic shell. Due to the finite thickness of the metallic shell, the sphere plasmon and the cavity mode interact, leading to a splitting of LSPR into two new LSPR: antibonding plasmon and symmetric plasmon. The antibonding coupling results in a higher energy mode (lower wavelength-shifted), while the bonding coupling corresponds to a higher wavelength-shifted LSPR peak. The coupling energy is proportional to a geometric parameter defined as the ratio between the inner and outer radii of the metallic shell. This means that the metallic shell thickness is associated with the interaction distance between two modes, in another word, the strength of the plasmon interaction. This phenomenon is therefore determined from the LSPR position. The Fe_3O_4@Ag core-shell NP system, shown in Figures 3 and 5, had the shifting of the LSPR position increase with a decrease in the geometric parameter, signifying that the mode coupling increased with a decrease in the geometric parameter. Therefore, the calculated results were in good agreement with the plasmon modes coupling theory. In addition, the calculated results agreed with the experimental results shown in Figure 2.

4. Conclusion

In summary, the optical properties of plasmonic nanostructures, mainly in terms of the optical absorption property of the Fe_3O_4@Ag core-shell NP, were studied using the DDA method. The calculated absorption spectra showed that both the Fe_3O_4 core size and the thickness of the Ag shell influenced the enhancement of the light absorption and the changes in the LSPR peak positions. Two absorption peaks appeared in each sample, left side and right side of the absorption peak of the pure Ag (382 nm). The Fe_3O_4 @Ag composite material is expected to be applicable in biomedicine, nanocatalysis, optic devices, and new functional devices in the future.

Acknowledgments

The authors are grateful to the Faculty of Applied Science and Engineering, Nong Khai Campus, Khon Kaen University for all facilities used. This work was partially supported by the Nanotechnology Center (NANOTEC), NSTDA, Ministry of Science and Technology, Thailand through its Center of Excellence Network program.

References

Arbab A. S., Bashaw, L. A., Miller B. R., Jordan E. K., Lewis B. K., Kalish H. and Frank J. A. 2003. Characterization of biophysical and metabolic properties of cells labeled with superparamagnetic iron oxide nanoparticles and transfection agent for cellular MR imaging. Radiology 229, 838-46.

Armelles, G., Alfonso Cebollada, A., García-Martín, A. and González, M. U. 2013. Magnetoplasmonics: Combining Magnetic and Plasmonic Functionalities. Advanced Optical Materials 1, 10-35.

Brollo, M. E. F., Lo´pez-Ruiz, R., Muraca, D., Figueroa, S. J. A., Pirota, K.R. and Knobel1, M. 2014. Compact Ag@Fe_3O_4 core-shell nanoparticles by means of single-step thermal decomposition reaction. Scientific Reports 4, 6839.

Chaiyachate, P. and Dasri, T. 2017. Optical Absorption and Scattering Properties of the Active Layer of Perovskite Solar Cells Incorporated Silver Nanoparticles. Oriental Journal of Chemistry 33, 807-813.

Choi, C. and Alivisatos, A. P. 2010. From artificial atoms to nanocrystal molecules: preparation and properties of more complex nanostructures. Annual Review of Physical Chemistry 61, 369-389.

Cunningham, J. C. H., Arai, T., Yang, P. C., McConnell, M. V., Pauly, J. M. and Conolly, S. M. 2005. Positive contrast magnetic resonance imaging of cells labeled with magnetic nanoparticles. Magnetic Resonance in Medicine 53, 999-1005.

Dani, R. K., Wang, H., Bossmann, S. H., Wysin, G. and Chikan, V. 2011. Faraday rotation enhancement of gold coated Fe_2O_3 nanoparticles: comparison of experiment and theory. The Journal of Chemical Physics 135, 224502.

Dasri, T. 2016. Theoretical calculation of plasmonic enhancement of silver nanosphere, nanocube, and nanorod embedded in organic solar cells. Integrated Ferroelectrics 175, 176-185.

Fontijn, W. F. J., Van der Zaag, P. j., Devillers, M. A. C., Brabers, V. A. M. and Metselaar, R. 1997. Optical and magneto-optical polar Kerr spectra of Fe_3O_4 and Mg^{2+}- or Al^{3+}-substituted Fe_3O_4. Physical Review B 56, 5432-5442.

Jain, P. K., Xiao, Y., Walsworth, R. and Cohen, A. E. 2009. Surface Plasmon Resonance Enhanced Magneto-Optics (SuPREMO): Faraday Rotation Enhancement in Gold-Coated Iron Oxide Nanocrystals. Nano Letters 9, 1644-1650.

Jiang, W., Zhou, Y., Xuan, S. and Gong, X. 2012. Superparamagnetic Ag@Fe_3O_4 core–shell nanospheres: fabrication, characterization and application as reusable nanocatalysts. Dalton Transactions 41, 4594-4601.

Johnson, P. B. and Christy, R. W. 1972. Optical Constants of the Noble Metals. Physical Review B 6, 4370-4379.

Kim, J., Lee, J. E., Lee, S. H., Yu, J. H., Lee, J. H., Park, T. G. and Hyeon, T. 2008. Designed Fabrication of a Multifunctional Polymer Nanomedical Platform for Simultaneous Cancer- Targeted Imaging and Magnetically Guided Drug Delivery. Advanced Materials 20, 478-483.

Lim, J., Eggeman, A., Lanni, F., Tilton, R. D. and Majetich, S. A. 2008. Synthesis and Single-Particle Optical Detection of Low-Polydispersity Plasmonic-Superparamagnetic Nanoparticles. Advanced Materials 20,

1721-1726.

Mahmoudi, M., Sant, S., Wang, B., Laurent, S. and Sen, T. 2011. Advanced Drug Delivery Reviews 63, 24-46.

Purcell, E. M. and Pennypacker, C. R. 1973. Scattering and Absorption of Light by Nonspherical Dielectric Grains. The Astrophysical Journal 186, 705.

Sheng-Nan, S., Chao, W., Zan-Zan, Z., Yang-Long, H., Venkatraman, S. S. and Zhi-Chuan, X. 2014. Magnetic iron oxide nanoparticles: Synthesis and surface coating techniques for biomedical applications. Chinese Physics B 23, 3, 037503.

Sompech, S., Thaomola, S. and Dasri, T. 2016. Optical Effects in the Active Layer of Organic Solar Cells with Embedded Noble Metal Nanoparticles. Oriental Journal of Chemistry 32, 85-91.

Sun. Y., Tian, Y., He, M., Zhao, Q., Chen, C., Hu, C. and Liu. Y. 2012. Controlled Synthesis of Fe_3O_4/Ag Core–Shell Composite Nanoparticles with High Electrical Conductivity. Journal of Electronic Materials 41, 519-523.

Prodan, E. and Nordlander, P. 2003. Structural Tunability of the Plasmon Resonances in Metallic Nanoshells. Nano Letters 3, 543-547.

Prodan, E. and Nordlander, P. 2004. Plasmon hybridization in spherical nanoparticles. The Journal of Chemical Physics 120, 5444-5454.

Yang, D., Pang, X., He, Y., Wang, Y., Chen, G., Wang, W. and Lin, Z. 2015. Precisely Size-Tunable Magnetic/Plasmonic Core/Shell Nanoparticles with Controlled Optical Properties. Angewandte Chemie International Edition 127, 12259-12264.